TOWARDS UNDERSTANDING INTERACTION BETWEEN HOT CARRIER AGEING AND PBTI

M. Duan, J. F. Zhang, Z. Ji, W. Zhang

Department of Electronics and Electrical Engineering, Liverpool John Moores University,
Byrom Street, Liverpool L3 3AF, UK
E-mail: j.f.zhang@ljmu.ac.uk

Abstract

Early works on device ageing often focus on one source, while devices in a circuit suffer degradation from different sources. There are only limited information on the impact of ageing from one source on ageing from a different source. This work researches into the interaction of ageing induced by Hot Carriers with that by Positive Bias Temperature Instability (PBTI). It will be shown that one can slow down the other and the ageing can be substantially overestimated without considering their interaction. Although a PBTI after Hot Carrier Ageing (HCA) will increase the degradation, a HCA following a PBTI can result in a reduction in ageing for long channel devices. The defect responsible for their interaction will be explored.

Introduction

There are a number of sources causing the ageing of MOSFETs, including Hot Carrier Ageing (HCA) [1-4], Positive/Negative Bias Temperature Instabilities (PBTI/NBTI) [4-12], and Time Dependent Dielectric Breakdown (TDDB) [13]. Early works typically investigate them separately and develop models without considering their interaction. For example, As-grown-Generation (AG) model has been proposed for NBTI [7-12] and PBTI [5,8] and power law based lifetime prediction has been used for HCA [1,2].

In real circuit operation, device ageing can be dominated by different sources under different operating conditions and ageing from one source can affect ageing from another source in the subsequent operation. For example, the access transistor of a Static Random Access Memory (SRAM) cell in Fig. 1a suffers from HCA during 'Read 0', as shown in Fig. 1b. The same transistor is subjected to PBTI stress in the subsequent 'Write 0' operation. At present, knowledge on the potential interaction between HCA and PBTI is limited [14] and the objective of this work is to research into it. It will be shown that one can slow down the other and ageing will be overestimated without considering this interaction.
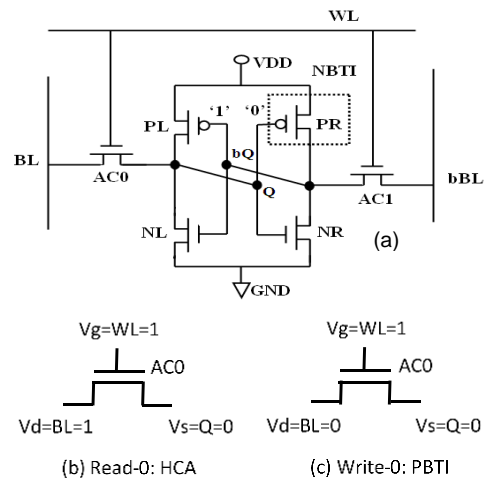
Fig. 1. (a) The six-transistor SRAM cell. (b) When 'Read 0', the access nMOSFET AC0 is under hot carrier ageing. (c) When 'Write 0', AC0 is under PBTI stress.

Devices and Experiments

nMOSFETs used in this work were fabricated by a commercial 28 nm CMOS process. They have metal gate and the high-k/SiON dielectric stack has an equivalent oxide thickness of 1.2 nm. To vary the relative strength of HCA versus PBTI, different channel lengths have been used, ranging from 27 to 225 nm. A relatively wide channel width of 900 nm is used to minimize the device-to-device variation [15].

PBTI was carried out with source and drain grounded, while HCA was under $V_g=V_d$. The ageing was monitored from the threshold voltage shift, measured under a given drain current of 100 nA $\times$ W/L [16]. All stresses and measurements were carried out at 125 ºC.

Over-estimation of ageing

If one assumes that HCA and PBTI are independent processes and there is no interaction between them, the total ageing will be the sum of HCA and PBTI (The symbol 'Δ' in Fig. 2a), which can be obtained by

performing HCA on one device and PBTI on another device.

To investigate the potential interaction, we used the waveform in Fig. 2b to stress one device alternately by HCA and PBTI. Fig. 2a shows that the ageing under the alternating HCA/PBTI stress (line) is considerably lower than the sum of HCA and PBTI. This conforms that HCA and PBTI affect each other and their interaction will be further investigated next.
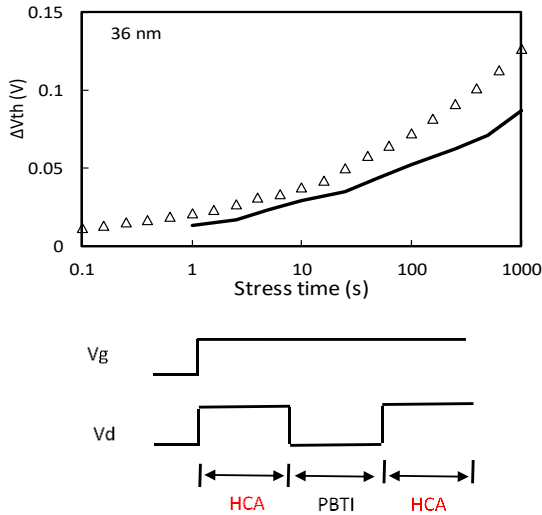
Fig. 2. (a) A comparison of HCA+PBTI (Symbol 'Δ'), when carried out independently on two different devices, with that when HCA and PBTI were carried out alternatively on the same device (the line). (b) Voltage waveforms for the line.

Interaction between PBTI and HCA

Fig. 3a shows the results when devices of different channel lengths were stressed by PBTI, HCA, and PBTI again in sequence. During the first PBTI, the ageing is independent of channel length, confirming that PBTI is a uniform process. As expected, the follow-on HCA is more severe for shorter channels, because of the higher lateral field over a shorter channel length for the same drain voltage. After HCA, the ageing during the 2nd PBTI becomes channel length dependent. To show this clearly, the HCA phase was removed in Fig. 3b and the two PBTIs were joined together. It can be seen that the shorter the channel, the less the 2nd PBTI ageing is. We conclude that HCA slows down the subsequent PBTI.

Fig. 4 shows the ageing following a sequence of HCA-PBTI-HCA. After HCA, PBTI ageing is more in longer channel device, in agreement with Figs. 3a&b. In the 2nd HCA post PBTI, ageing increases for the short channel device, but decreases for the long channel device. To explain this behavior, we study the defects responsible for the ageing next.
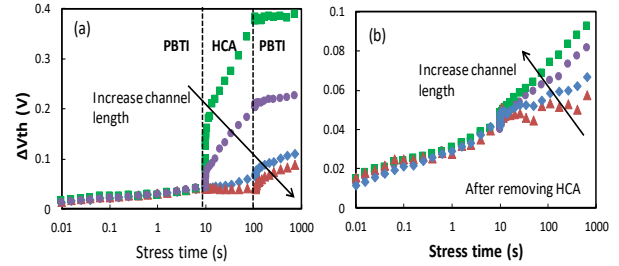
Fig. 3. (a) Ageing under a stress sequence of PBTI, HCA, and PBTI for different channel lengths. (b) A replot of (a) by removing the HCA phase.
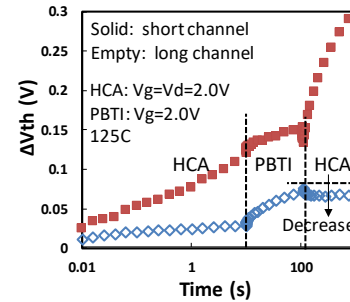
Fig. 4. Ageing under a stress sequence of HCA, PBTI, and HCA for different channel lengths.

Defects

Fig. 5 shows that the ΔVth is cyclic-able by alternating the gate bias polarity, when the PBTI Vg is relatively low at +1.5 V. After a trap captures an electron, the trapping is not permanent and it can be detrapped. This type of traps are referred to as 'Cyclic Electron traps (CET)'.

When stress voltage increases to Vg=+2.0 V, ΔVth is higher, as expected. The amount of CET is also higher. Moreover, some traps can remain charged at the end of the discharge phase and they are called as 'anti-neutralization electron traps (ANET)'. Based on this understanding of defects, we explain the interaction between PBTI and HCA observed in Figs. 3 and 4 next.

Physical processes

In Fig. 3, HCA can charge some of the ANET. As these ANET is already charged, they are not available in the subsequent PBTI. The shorter the channel, the more ANET is charged by HCA, so that the less the ageing in the subsequent PBTI, as shown in Fig. 3b. This indicates that the same ANET can be charged by either HCA or PBTI.

The reduction for the longer channel device during the 2nd HCA in Fig. 4 is caused by detrapping of CET. As illustrated by Fig. 6, the vertical electrical field is

progressively reduced when moving from the source towards the pinch-off point during HCA. Some CET charged under higher vertical field during the PBTI can be detrapped during HCA. For shorter channel, HCA is strong and over-compensates the detrapping. For longer channel, HCA is too weak to compensates the detrapping, leading to the observed reduction in ageing.
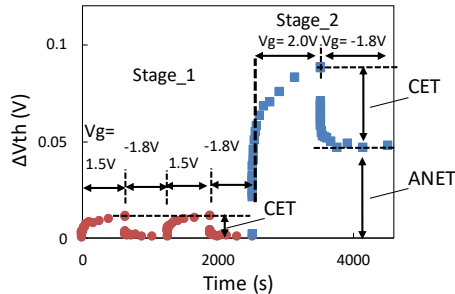
Fig. 5. In the stage 1, the cyclic electron traps (CET) can be charged by PBTI at Vg=+1.5 V and discharged under Vg=-1.8 V. In the stage 2, PBTI was under Vg=+2 V. CET increases and the anti-neutralization electron traps (ANET) remain charged at the end of discharge phase.
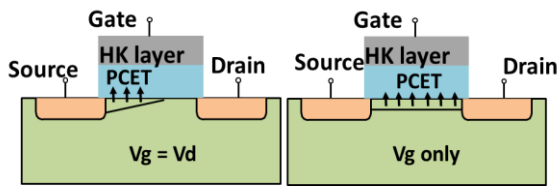
Fig. 6. An illustration of the reduction of vertical oxide field between source and pinch-off point during HCA, when compared with PBTI.

Conclusions

The interaction between PBTI and HCA is investigated in this work. It is shown that one can slow down the other substantially and the overall ageing will be overestimated without considering this interaction. Although PBTI is uniform without HCA, it becomes channel-length dependent after HCA. HCA can pre-charge the traps, making them unavailable to the subsequent PBTI.

For long channel devices, ageing during HCA after PBTI can even reduce. This is because the reduction of vertical field between source and pinch-off point during HCA results in a partial detrapping of the cyclic electron traps filled by the preceding PBTI.

Acknowledgements

The authors thank D. Vigar for supply of test

References

[1] C. Hu, S. C. Tam, F. C. Hsu, P. K. Ko, T. Y. Chan, and K. W. Terrill, IEEE Trans. Elec. Dev., Vol. ED-32, pp. 375–385, 1985.

[2] M. Duan, J. F. Zhang, A. Manut, Z. Ji, W. Zhang, A. Asenov, L. Gerrer, D. Reid, H. Razaidi, D. Vigar, V. Chandra, R. Aitken, B. Kaczer, and G. Groeseneken, Proc. IEDM, pp. 547-550, 2015.

[3] M. Duan, J. F. Zhang, Z. Ji, W. Zhang, B. Kaczer, and A. Asenov IEEE Trans. Elec. Dev., Vol. 64, pp. 2478–2484, 2017.

[4] M. Duan, J. F. Zhang, Z. Ji, W. Zhang, D. Vigar, A. Asenov, L. Gerrer, V. Chandra, R. Aitken, and B. Kaczer IEEE Trans. Elec. Dev., Vol. 63, pp. 3642-3648, 2016.

[5] R. Gao, Z. Ji, J. F. Zhang, J. Marsland, and W. D. Zhang, IEEE Trans. Elec. Dev., Vol. 65, pp. 3662–3668, 2018.

[6] B. Kaczer, T. Grasser, P. J. Roussel, J. Franco, R. Degraeve, L. A. Ragnarsson, E. Simoen, G. Groeseneken, and H. Reisinger, Proc. IRPS, pp. 26-32, 2010.

[7] J. F. Zhang, Z. Ji, and W. Zhang, Microelectronics Reliability, Vol. 80, pp. 109–123, 2018.

[8] R. Gao, Z. Ji, S. M. Hatta, J. F. Zhang, J. Franco, B. Kaczer, W. Zhang, M. Duan, S. De Gendt, D. Linten, G. Groeseneken, J. Bi and M. Liu, Proc. IEDM, pp. 778-781, 2016.

[9] Z. Ji, S. F. W. M. Hatta, J. F. Zhang, J. G. Ma, W. Zhang, N. Soin, B. Kaczer, S. De Gendt, and G. Groeseneken, Proc. IEDM, pp. 413-416, 2013.

[10] M. Duan, J. F. Zhang, Z. Ji, W. Zhang, B. Kaczer, T. Schram, R. Ritzenthaler, A. Thean, G. Groeseneken, and A. Asenov, Proc of Symp. VLSI Technol., pp.74-75, 2014.

[11] R. Gao, A. B. Manut, Z. Ji, J. Ma, M. Duan, J. F. Zhang, J. Franco, S. W. M. Hatta, W. Zhang, B. Kaczer, D. Vigar, D. Linten, and G. Groeseneken, IEEE Trans. Elec. Dev., Vol. 64, pp. 1467–1473, 2017.

[12] R. Gao, Z. Ji, A. B. Manut, J. F. Zhang, J. Franco, S. W. M. Hatta, W. D. Zhang, B. Kaczer, D. Linten, and G. Groeseneken, IEEE Trans. Elec. Dev., Vol. 64, pp. 4011–4017, 2017.

[13] W. D. Zhang, J. F. Zhang, C. Z. Zhao, M. H. Chang, G. Groeseneken, and R. Degraeve, IEEE Electron Dev.Lett., vol.27, no.5, pp.393-395, 2006.

[14] M. Duan, J. F. Zhang, J. C. Zhang, W. Zhang, Z. Ji, B. Benbakhti, X.F. Zheng, Y. Hao, D. Vigar, V. Chandra, R. Aitken, B. Kaczer, G. Groeseneken and A. Asenov, Proc. IRPS, pp. XT-5.1-XT.5.7, 2017.

[15] M. Duan, J. F. Zhang, Z. Ji, W. D. Zhang, B. Kaczer, T. Schram, R. Ritzenthaler, G. Groeseneken, and A. Asenov, IEEE Trans. Elec. Dev., Vol. 61, pp. 3081–3089, 2014.

[16] M. Duan, J. F. Zhang, Z. Ji, J. G. Ma, W. Zhang, B. Kaczer, T. Schram, R. Ritzenthaler, G. Groeseneken, and A. Asenov, Proc. IEDM, pp. 774-777, 2013.